



UNIVERSITY OF LEEDS

This is a repository copy of *The Application of a Geographically Weighted Principal Component Analysis for Exploring Twenty-three Years of Goat Population Change across Mongolia*.

White Rose Research Online URL for this paper:
<http://eprints.whiterose.ac.uk/115651/>

Version: Accepted Version

Article:

Tsutsumida, N, Harris, P and Comber, A orcid.org/0000-0002-3652-7846 (2017) The Application of a Geographically Weighted Principal Component Analysis for Exploring Twenty-three Years of Goat Population Change across Mongolia. *Annals of the American Association of Geographers*, 107 (5). pp. 1060-1074. ISSN 2469-4452

<https://doi.org/10.1080/24694452.2017.1309968>

© 2017 by American Association of Geographers. This is an Accepted Manuscript of an article published by Taylor & Francis in *Annals of the American Association of Geographers* on 31 May 2017, available online:
<http://www.tandfonline.com/10.1080/24694452.2017.1309968>.

Reuse

Items deposited in White Rose Research Online are protected by copyright, with all rights reserved unless indicated otherwise. They may be downloaded and/or printed for private study, or other acts as permitted by national copyright laws. The publisher or other rights holders may allow further reproduction and re-use of the full text version. This is indicated by the licence information on the White Rose Research Online record for the item.

Takedown

If you consider content in White Rose Research Online to be in breach of UK law, please notify us by emailing eprints@whiterose.ac.uk including the URL of the record and the reason for the withdrawal request.



eprints@whiterose.ac.uk
<https://eprints.whiterose.ac.uk/>

1

2 **Title:** The application of a geographically weighted principal components analysis for
3 exploring 23 years of goat population change across Mongolia

4

5 **Author names/Affiliations:**

6 Narumasa Tsutsumida¹, Paul Harris², Alexis Comber³

7 ¹ Graduate School of Global Environmental Studies, Kyoto University,

8 Yoshida-honmachi, Sakyo, Kyoto, Kyoto, JP 606-8501

9 ² Rothamsted Research, North Wyke, Okehampton, Devon, UK EX20 2SB

10 ³ School of Geography, University of Leeds, Leeds, UK LS2 9JT

11 **Abstract**

12 The dzud are extreme weather events in Mongolia of deep snow, severe cold, or
13 other conditions that render forage unavailable or inaccessible, which in turn, result in
14 extensive livestock deaths. Mongolia is economically vulnerable to extreme events
15 due to an increase in non-professional herders and the livestock population, that a
16 de-regularised industry has brought about. Thus it is hugely informative to try to
17 understand the spatial and temporal trends of livestock population change. To this
18 end annual livestock census data are exploited and a geographically weighted
19 principal components analysis (GWPCA) is applied to goat data recorded from 1990
20 to 2012 in 341 regions. This application of GWPCA to temporal data is novel and is
21 able to account for both temporal and spatial patterns in goat population change.
22 Furthermore, the GWPCA methodology is extended to simultaneously optimise the
23 number of components to retain and the kernel bandwidth. In doing so, this study not
24 only advances the GWPCA method but also provides a useful insight into the
25 spatio-temporal variations of the Mongolian goat population.

26

27

28 **Keywords**

29 Spatio-temporal; GWmodel; Livestock; Grasslands; Sustainability

30

For Peer Review Only

31 **Introduction**

32 It is important to evaluate the impacts of disasters to improve and support
33 agricultural planning. In Mongolia, deep snow, severe cold and associated conditions,
34 called *dzud*, occur repeatedly and make forage unavailable or inaccessible to
35 livestock. This results in high livestock mortality (Fernandez-Gimenez, Batbuyan, and
36 Baival 2012; Fernández-Giménez et al. 2015) and huge economic losses, as
37 livestock in Mongolia represents 16% of national GDP (UNDP and NEMA 2010).
38 Traditional nomadic pastoralism is one of the most sustainable ways of life on
39 grasslands and sparsely vegetated lands, as are commonly found in Mongolia
40 (Millennium Ecosystem Assessment 2005; Research Institute for Humanity and
41 Nature 2012). Vegetation availability depends on the impacts of livestock grazing
42 which has been well managed by nomadic herders over thousands of years
43 (Research Institute for Humanity and Nature 2012), and is not suited to intensive
44 livestock and crop production. In particular, excessive livestock populations, whether
45 managed commercially or traditionally, endangers sustainability (Geist and Lambin
46 2004; Suttie, Reynolds, and Batello 2005). Recent changes to the Mongolian
47 livestock industry, which has become swamped with non-professional herders due to

48 de-regularisation, has made the grasslands vulnerable to environmental change and
49 to extreme weather events. Thus there is a clear need to understand the
50 spatio-temporal trends in Mongolia's livestock populations, accounting for the impacts
51 of the dzuds.

52 Data on livestock populations (sheep, goat, horse, cattle and camel) are
53 collected for 341 regions (a second administrative subdivision level, called *soum*) in
54 Mongolia by the official statistics service. For this study, goat data for a 23 year period
55 1990-2012, covering two devastating dzuds during 2001-2 and 2009-10, was
56 analysed. A geographically weighted principal components analysis (GWPCA) was
57 used with the aim of generating spatio-temporal insights about goat populations,
58 particularly for abrupt changes caused by dzuds. A standard principal components
59 analysis (PCA) provides a useful starting point to reduce the dimensionality of the
60 temporally-indexed goat data and to observe major trends. However, PCA ignores
61 any spatial structure in the data (Demšar et al. 2013), whilst GWPCA is explicitly
62 designed to do so (Fotheringham, Brunsdon, and Charlton 2002; Lloyd 2010; Harris,
63 Brunsdon, and Charlton 2011; Harris et al. 2015).

64 GWPCA constructs local PCAs from subsets of the data under a moving
65 window or kernel where the data are weighted by their distance to the kernel centre.
66 Critical factors in the operation of GWPCA are the specification of the kernel
67 bandwidth, which controls the degree of localness, and choosing the number of
68 components to retain (NCR). Bandwidth optimization routines exist, but are
69 dependent on the NCR value, that has to be pre-specified (Harris et al. 2011; 2015).
70 This paper addresses this technical limitation of GWPCA and proposes two novel
71 methods to determine the bandwidth and NCR value simultaneously. In doing so, a
72 better understanding of the spatio-temporal dynamics of the Mongolian goat
73 populations in relation to the duzds is provided.

74 This article is organised as follows. Firstly, background information on
75 Mongolian livestock populations is presented, together with introductions to PCA and
76 GWPCA. Secondly, the study data is described. Thirdly, PCA and the GWPCA
77 methodology are formally presented. Fourthly, the results of applying PCA and
78 GWPCA to the goat population data are given, including the outcomes of the dual
79 bandwidth and NCR optimisations for GWPCA. Finally, a summary, discussion and
80 concluding remarks section is given.

81

82 **Background**83 Livestock populations in Mongolia

84 Nomadic pastoralism has provided a sustainable way of life for thousands of
85 years in Mongolia (Research Institute for Humanity and Nature 2012). Although
86 Mongolian grasslands have been well-managed, there are concerns about the
87 impacts of increases in livestock populations. The lives of nomadic pastoralists have
88 been strongly influenced by political changes, especially the move from a planned
89 economy to a free-market economy in 1992 (Fernandez-Gimenez 2006). Prior to this,
90 livestock production was managed centrally and nomadic herders raised state-owned
91 livestock, restricting excessive livestock production. The government encouraged
92 herders to organize their collectives locally, and gave salaried (professional) herders
93 the responsibility of breeding livestock. Collectives were self-regulated in their land
94 use and their seasonal long-distance travel, resulting in good pasture maintenance
95 with advance preparedness for keeping livestock secure from extreme events
96 (Fernandez-Gimenez 2006). Since the transition to a free-market economy, pastures
97 have been managed by individual herders, leading to serious sustainability and land

108 management issues, as herders are now focussed on profit and their number has
109 more than doubled (Togtokh 2008) – all of which makes the livestock industry more
110 vulnerable. Five main livestock types are found in Mongolia (sheep, goat, horse,
111 cattle and camel), and the country-wide goat population has rapidly increased since
112 the government policy change in 1992 (Figure 1). This increase is primarily due to the
113 strong demand for goat cashmere (Saizen, Maekawa, and Yamamura 2010), but
114 unfortunately, the rate of increase threatens livestock sustainability and the nomadic
115 lives of herders.

116 Livestock losses occur during periods of the dzud as a result of deep snow and
117 severe cold (Fernandez-Gimenez, Batbuyan, and Baival 2012; Tsutsumida and
118 Saizen 2014). Additional pressure is also placed on herders as the dzud directly
119 results in reduced opportunities for grazing in the summer that follows, as a result of
120 droughts. Effects of this combination of winter dzuds and summer droughts can be
121 seen in Figure 1 for the years 2001-2 and 2009-10, where declines in the sheep and
122 goat populations are clearly evident. As a result of the 2009-10 dzud, approximately
123 20% of the country's livestock population were killed, affecting 28% of Mongolia's
124 human population (Fernandez-Gimenez, Batbuyan, and Baival 2012;

115 Fernández-Giménez, Batkhisig, and Batbuyan 2012). The increase in
116 non-professional herders, with limited knowledge in traditional herding, has
117 compounded this livestock loss in the dzud years (UNDP and NEMA 2010).

118 Little attention has been paid into the geographical dynamics of the Mongolian
119 livestock population, over this 23-year period of change. Although some research has
120 been conducted, notably by Saizen, Maekawa, and Yamamura (2010) who found
121 areas of goat population increase to be independent of land cover. Saizen, Maekawa,
122 and Yamamura (2010) also noted that in more severe conditions, goat herders were
123 not restricted to the grazing pastures close to Ulaanbaatar, as goats are more
124 resilient to severe conditions, and the fact that a key goat product, cashmere, is
125 relatively portable. Liu et al. (2013) investigated the relationship between goat
126 population density and various climatic factors and suggested that the marked
127 increase in goat population density was a key non-climatic factor affecting grassland
128 degradation. Hilker et al. (2014) observed that livestock population increases,
129 associated with vegetation greenness, were primarily in the western part of Mongolia.
130 Thus previous research has tended to focus on environmental issues and not the
131 vulnerability of the livestock populations due to dzuds, even though they are relatively

132 common. This study seeks to address this oversight by investigating the
133 spatio-temporal pattern of goat population change in relation to the varying impacts of
134 dzuds, via a GWPCA approach.

135

136 PCA and geographically weighted PCA

137 PCA is standard information reduction technique, commonly employed in many
138 areas of data analysis. It transforms a set of m correlated variables into a new set of
139 m uncorrelated variables called components. The components are linear
140 combinations of the original variables and can allow for a better understanding of
141 differing sources of variation and key trends in data. Its use as a dimension reduction
142 technique is viable if the first few components account for most (say, 80 to 90%) of
143 the variation in the original data. Component scores and component loadings data
144 are produced, where the latter display how much each of the original variables
145 attribute to the dimensional variance of the overall data. For details, see Jolliffe
146 (2002).

147 There are a number of ways that a PCA can be usefully applied to multivariate
148 spatio-temporal data sets, such as the livestock data sets for this study (when all five

149 livestock types are considered). Demšar et al. (2013) provide a review in this respect,
150 where the many dimensional groups can be treated in a variety of ways. This study
151 applies a PCA to the goat population data, collected over a 23-year time period. Thus
152 the application of PCA is to a set of 23 time-stamped geographic variables, where
153 each variable measures goat population for a different year. This means that the PCA
154 only accounts for the temporal correlations in the data.

155 PCAs have been used to identify spatio-temporal data characteristics in many
156 scientific fields (e.g. Felipe-Sotelo et al. 2006; Lasaponara 2006; and see Demsar et
157 al. 2013 therein). For example, Lasaponara (2006) applied PCA for the evaluation of
158 vegetation anomalies from multi-temporal remote sensing data; and found that the
159 first principal component (PC1) related to a general vegetation distribution pattern,
160 while the second (PC2) indicated a decreasing trend of vegetation amount. In the
161 atmospheric sciences, PCAs are commonly applied to spatio-temporal (univariate)
162 data, and is referred to as an empirical orthogonal function (EOF) analysis (e.g.
163 Obled and Creutin (1986)). However for EOFs, the time series data is sufficiently long
164 enough to consider PCA in Q-mode (rather than the usual R-mode), thus spatial
165 correlations are captured as the data matrix is transposed. If the livestock population

166 data of this study was considered temporally long enough (i.e. collected over 100
167 years, say), then such an application of Q-mode PCA could also have been
168 considered. Instead, an R-mode PCA is applied and thus only temporal correlations
169 in the goat data are captured. Note that applications of PCA to spatio-temporal data
170 entails that Q-mode PCA is often referred to as S-mode PCA, where "S" denotes
171 spatial, and R-mode PCA is often referred to as T-mode PCA, where "T" denotes
172 temporal. The idea being that Q-mode and R-mode PCAs are reserved for attribute
173 sub-space applications with no spatio-temporal context.

174 However, a standard (R-mode) PCA application to this study's goat data does
175 not account for any spatial effects, because it only ensures a non-spatial linear
176 transform (Demšar et al. 2013). In order to deal with such a naïve application, but
177 from a spatial effects point of view only, GWPCA can be used. This adaptation of
178 PCA provides a better description of any spatial phenomenon in the structure of the
179 data. It uses a moving window weighting technique and constructs a localized PCA at
180 all target locations (e.g. a grid, such as the application by Comber, Harris, and
181 Tsutsumida (2016)). It is important to note, that although spatio-temporal correlations
182 in the goat population data are captured via GWPCA, only spatial dependencies in

183 the data are fully captured. Temporal dependencies such as those between
184 neighbouring years, are not fully captured nor are true spatio-temporal dependencies.
185 That requires a further extension to GWPCA to a full spatio-temporal approach,
186 similar that proposed for GW regression by Huang, Wu, and Barry (2010). Thus in
187 this study, both PCA and GWPCA are applied in order to provide a better
188 understanding of the dynamics of the Mongolian goat population data, at a
189 soum-level scale, across the period 1990–2012.

190

191 **Study data**

192 Annual livestock population data were obtained from the National Statistical
193 Office (NSO) of Mongolia for the period 1990–2012. Populations were summarized
194 per soum, an administrative sub-division area. Since local governments collect taxes
195 from herders according to herd size, the data are assumed to reflect livestock
196 numbers reasonably well (Saizen, Maekawa, and Yamamura 2010). Administrative
197 boundaries slightly changed during the 23-year study period. To cater for this, the
198 data were merged accounting for all 341 soums, using the most recent boundaries.
199 Thus all data are taken into account when a soum changed or was incorporated into a

200 neighbour. Missing data that arose because of these changes, were infilled using a
201 probabilistic PCA method provided in the pcaMethod R package (Stacklies et al.
202 2007). This infilling was fairly minor and was not considered an issue for subsequent
203 analyses.

204 As would be expected, the goats data are highly correlated, especially across
205 adjacent years as shown in Figure 2, with the weakest correlations between the dzud
206 year of 2002 and all others, and the dzud year of 2010 and all others. Intuitively, this
207 correlation analysis for the temporally-indexed goats data, directly implies that goat
208 population change does not increase or decrease at the same rate across all 341
209 soums. This in turn, provides some insight into the expected value of a spatial
210 analysis of the goats data, via a GWPCA.

211

212 **Methods**

213 Principal components analysis (PCA)

214 Given an $n \times m$ dimensional data matrix X , a PCA to this data consists of
215 conducting this transformation:

$$216 \quad L V L^T = S \quad (1)$$

217 where L is the matrix of eigenvectors with $n \times m$ dimension, V is the diagonal
218 matrix of eigenvalues, and S is the variance–covariance matrix with $m \times m$
219 dimension. V indicates the eigenvalues of the PCs, representing the axes of a new
220 dimension. Each column of L represents the loadings corresponding to a PC. The
221 PCs are ordered according to the size of eigenvalues, meaning that PC1 corresponds
222 to the largest eigenvalue, and PC2 corresponds to the second largest, and so on.
223 Transformed component scores in matrix T is represented by

$$224 \quad T = XL \quad (2)$$

225 where T consists of a linear combination of the original values, which in this study is
226 the multi-temporal goat population data with $n = 341$ and $m = 23$.

227

228 Geographically weighted principal components analysis (GWPCA)

229 A GWPCA utilises a kernel weighting approach where localised PCs are found
230 at target locations. At a target location, neighbouring observations are weighted by a
231 distance-decay weighting function, and then a standard PCA is locally applied to its
232 own specific weighted data subset. The size of the window over which this localised
233 PCA might apply is controlled by the kernel's bandwidth. Small bandwidths lead to

234 more rapid spatial variation in the results whereas large bandwidths yield results
 235 increasingly close to the global PCA solution. This study identifies an adaptive
 236 bandwidth corresponding to a bi-square kernel, a discontinuous function that
 237 generates distance-decaying weights data points within the set bandwidth.
 238 Observations outside of the bandwidth's range receive weights of zero, and hence
 239 the discontinuity. For details, see Gollini et al. (2015).

240 Thus for coordinates (u, v) at spatial location i , GWPCA involves the
 241 conception that the goat population time series variables x_i have a certain
 242 dependence on their locality where $\mu_{(u,v)}$ and $\Sigma_{(u,v)}$, are the GW mean vector and
 243 the GW variance–covariance matrix, respectively. This GW variance–covariance
 244 matrix is calculated by

$$245 \quad \Sigma_{(u,v)} = X^T W_{(u,v)} X \quad (3)$$

246 where $W_{(u,v)}$ is a diagonal matrix of geographical weights that are generated by the
 247 chosen kernel weighting function. The GWPCA at spatial location i can be
 248 computed using

$$249 \quad L V L^T |_{(u_i, v_i)} = \Sigma_{(u_i, v_i)} \quad (4)$$

250 where $\Sigma(u_i, v_i)$ is the GW variance-covariance at that location. The scores matrix at
251 the same location can be found using $T(u_i, v_i) = XL(u_i, v_i)$. On dividing each local
252 eigenvalue by $tr(V(u_i, v_i))$, localized versions of the proportion of the total variance
253 (PTV) in the original data accounted for by each component can be found. Thus at
254 each of the 341 sums of this study (i.e. the target locations), a GWPCA provides 23
255 components, 23 eigenvalues, a component loadings set of size 341×23 , and a
256 component scores set of size 341×23 .

257 Bandwidth selection is crucial for the application of any GW model. For GWPCA,
258 bandwidth selection can be guided by a 'leave-one-out' residual (LOOR) approach,
259 where scores data are assessed for goodness of fit (GoF) against observed data. The
260 optimal bandwidth is one that corresponds to LOOR data that provides the smallest
261 GoF statistic. This cross-validation procedure and extensive commentaries on
262 choosing bandwidths are provided in Harris et al. (2015). Of note is that the NCR
263 value is decided upon a priori and an optimal bandwidth cannot be found if all m
264 components are retained. Thus the results of this residual-based bandwidth selection
265 procedure are somewhat dependent on a user-specified value of NCR. To counter
266 this dependency, this study proposes two alternative techniques to determine the

267 bandwidth and the NCR value, concurrently. These methodological advances are
 268 described and implemented below.

269

270 Geographically weighted correlation analysis

271 A GW correlation analysis (Harris and Brunsdon 2010) on the outputs from the
 272 PCA with the raw data is also conducted. Here for variables x and y at spatial
 273 location i where the geographical weights w_{ij} again accord to a bi-square function,
 274 definitions for a GW standard deviation and a GW correlation coefficient, are
 275 respectively

$$276 \quad s(x_i) = \sqrt{\frac{\sum_{j=1}^n w_{ij} (x_j - m(x_i))^2}{\sum_{j=1}^n w_{ij}}} \quad (5)$$

277 and

$$278 \quad \rho(x_i, y_i) = \frac{c(x_i, y_i)}{(s(x_i)s(y_i))} \quad (6)$$

279 , where a GW mean is

$$280 \quad m(x_i) = \frac{\sum_{j=1}^n w_{ij} x_j}{\sum_{j=1}^n w_{ij}} \quad (7)$$

281 and a GW covariance is

$$c(x_i, y_i) = \frac{\sum_{j=1}^n w_{ij} \{(x_j - m(x_i))(y_j - m(y_i))\}}{\sum_{j=1}^n w_{ij}} \quad (8)$$

Throughout this study, GWPCA and GW correlations use functions (or adapted functions) from the GWmodel R package (Gollini et al. 2015).

285

286 **Results**

287 The global PCA

In order to understand any GW model output, it is always important to fit the usual global model for context. In this respect, a PCA was conducted on the 23 temporal variables describing goat populations. Table 1 shows that the first two PCs have eigenvalues greater than unity, and for these two PCs, the cumulative PTV exceeds 90%. This implicitly assumes a uniform temporal trend in goat population across all 341 sums over the 23-year period. The PCA loadings given in Table 2 indicate that the five of the most influential years are 1996-1999 and 2001 for PC1; 1990-1991 and 2010-2012 for PC2.

296

297 A GW correlation analysis on the PCA scores and raw data

298 As the component loadings in Table 2 are the (global) correlation coefficients
299 between the component scores and the raw data, a GW correlation analysis on this
300 data can be used to investigate whether the correlations change across study region.
301 Figure 3 maps the GW correlations between the PCA scores data for PC1 to PC3,
302 and the raw data from the three most influential years. The GW correlations were
303 found using a user-specified bandwidth of 10% (i.e. each local correlation uses the
304 nearest 34 data pairs). As would be expected, spatial coherence for such correlations
305 is highest for PC1, but diminishes through PC2 to PC3. This suggests that the PCA is
306 missing some spatial structure in the data, and as such, an application of GWPCA is
307 worthwhile. Intuitively, this is expected, as the spatio-temporal trend in goat
308 populations is not expected to be uniformly the same across all of Mongolia (as
309 similarly suggested for observations made above, with respect to Figure 2).

310

311 GWPCA calibration with dual bandwidth and NCR optimization

312 As outlined above, in order to calibrate a GWPCA, first the NCR value needs to
313 be user-specified and only then, can an optimal GWPCA bandwidth be found via
314 cross-validation. In previous GWPCA studies, NCR is commonly chosen according to

315 a 80% or 90% threshold of the cumulative PTV from the global PCA. Thus in this
316 study, NCR = 1 or 2 would be appropriate (see Table 1). This bandwidth selection
317 approach is far from ideal, as can be seen in Table 3, where different 'optimal'
318 bandwidths (found by the cross-validation procedure) simply correspond to different
319 choices of NCR (in this case, NCR values from 1 to 10). Furthermore, the results
320 suggest a tendency to a global PCA process for the study data, as eight out of ten
321 bandwidths are taken at 341 suggesting a kernel bandwidth that contains all of the
322 soums data. If this is truly the case (see note 1), then there appears no value in
323 applying GWPCA, and the localized analysis should cease at this juncture.

324 However, the choice of bandwidth can be investigated more deeply. This is
325 because the results presented in Table 3 are not directly comparable, as given
326 'optimal' bandwidths correspond to minimized GoF statistics (not shown) where the
327 NCR-specific LOOR data sets have been summarized by their mean. To ensure that
328 the minimized GoF statistics are comparable across different values of NCR, the
329 LOOR data can be summarized instead by their coefficient of variation (CoV) to
330 provide relative (and thus comparable) GoF statistics for each bandwidth and for
331 each NCR value. This leads to a dual optimization approach as shown in Figure 4(i),

332 where the aim to concurrently find the bandwidth and the NCR value that
333 corresponds to minimum GoF (LOOR CoV) value. Again considering only NCR
334 values from 1 to 10, and a clear minimum GoF is reached at 1.296 corresponding to a
335 bandwidth of 247 nearest neighbours and an NCR value of 5. Each individual line in
336 the plot of Fig 4(i) corresponds to a different bandwidth choice, from 5 to 341. This
337 constitutes the first extension to the existing bandwidth selection procedure.

338 A second alternative is to transfer the usual cumulative PTV approach for NCR
339 selection to a local setting. Globally, a user-specified choice of NCR = 1 or 2 is based
340 on the global cumulative PTV scree plot (e.g. Varmuza and Filzmoser (2009)). This
341 approach can be transferred locally using the local cumulative PTV data from each
342 local PCA from a series of GWPCAs. Local cumulative PTV data were calculated
343 from GWPCAs calibrated with bandwidths ranging from 10 to a maximum of 341 and
344 the resultant local scree plots are depicted in Figure 4(ii). Clearly, the local scree plots
345 suggest that NCR = 2 is the point when some of the local cumulative PTV data
346 exceeds a 90% threshold. Given this, NCR = 2 again appears appropriate for a
347 GWPCA calibration. However, the bandwidth is still required, and unlike the existing
348 approach a bandwidth is identified that has the smallest GoF (LOOR mean) value,

349 but crucially also corresponds to a localized cumulative PTV value exceeding 90%
350 (for all NCR = 2). This indicates a relative tight bandwidth of 198 nearest neighbours.

351 Thus in summary, there are three possible bandwidths for GWPCA calibration:

352 (a) 341 (via NCR = 1 or 2); (b) 247 (via NCR = 5); and (c) 198 (via NCR = 2). All three
353 should be considered as entirely valid, but where approach (a), the existing approach,
354 strongly suggests a stationary process with respect to a PCA. Given that approach
355 (a) has drawbacks, not only with respect to NCR/bandwidth specification, but also
356 (indirectly) due to current limitations in the GWPCA code (see note 1), it is dropped in
357 favour of the two newly proposed approaches (b and c) which are both viewed as a
358 methodological advance. In the spirit of spatial exploration, which all GW models are
359 eminently designed for, both approaches were investigated further all of the
360 subsequent GWPCA outputs described below are specified with either: (i) a
361 bandwidth of 247 via a NCR value of 5; or (ii) a bandwidth of 198 via a NCR value of
362 2.

363

364 PCA versus GWPCA results

365 GWPCA is now applied to account for expected spatial heterogeneity in the
366 annual goat population data during 1990-2012 with: (i) a bandwidth of 247 via a NCR
367 value of 5 (call this 'GWPCA-A'); and (ii) a bandwidth of 198 via a NCR value of 2 (call
368 this 'GWPCA-B'). The GWPCA results are compared with those from global PCA,
369 throughout. To compare GWPCA-A, GWPCA-B, and PCA, only the first two
370 components (PC1 and PC2) from each calibration are considered. Observe that once
371 a bandwidth is defined, local components up until any NCR value (in this case NCR =
372 23) can actually be found and investigated. So in this respect, the NCR values of 2
373 and 5 from the bandwidth selection procedure do not have to pervade the remainder
374 of the analysis (e.g. Harris et al. 2015).

375

376 Scores data

377 PC1 and PC2 scores from GWPCA-A, GWPCA-B, and the global PCA are
378 mapped in Figure 5. Observe that for GWPCA, a full, $n = 341$ valued scores data set
379 is available at each location, for each component. Thus, the GWPCA scores data that
380 are mapped are only those that fully correspond to their location. PC1 scores of
381 GWPCA-A and GWPCA-B correlate with those from the global PCA, with $r = 0.846$

382 and $r = 0.742$, respectively. PC2 scores of GWPCA-A and GWPCA-B correlate with
383 those from the global PCA, with correlations of $r = 0.943$ and $r = 0.872$,
384 respectively. These moderate to strong correlations simply reflect the relatively large
385 bandwidth sizes used, and such correlations would tend to unity as the bandwidth
386 increases. However these global correlations hide spatial detail, where the study's
387 aim is to see where the local spatial structure in the temporally-changing goat
388 population (via the GWPCA outputs) differs to that found globally (via the PCA
389 outputs). In this respect, the clearest regional differences in both the PC1 and PC2
390 scores data appear in the north-eastern regions of Mongolia, bordering Russia and
391 also the south-western regions bordering China. Thus the temporal dynamics of goat
392 population change is likely to be clearly different in these regions to that expected
393 nationally.

394

395 Percentage PTV data

396 Globally, the PTV for PC1, and the cumulative PTV for PC1 and PC2 combined,
397 are 84% and 92%, respectively. This suggests a high correlation amongst the goat
398 population data, year on year, throughout the 23-year period. However, the global

399 PTV values (from PCA) implicitly assume that such relationships are constant across
400 Mongolia - with relatively uniform changes in goat populations everywhere. Mapping
401 the corresponding localized PTV outputs from GWPCA shows where this is the case,
402 and the degree to which it is not (Figure 6).

403 Focusing on the third row only of Figure 6, regionally the temporal trend in goat
404 population change is actually more uniform than that found globally in central
405 northern regions (coloured dark green), where local PTV data are higher. Conversely,
406 the temporal trend in goat population change is actually less uniform than that found
407 globally in western regions (coloured dark pink), where local PTV data is lower.

408 These changes in regional behaviour broadly confirms that observed for the scores
409 data, above. The PTV maps in the first and second rows of in Figure 6 provide detail
410 of the component contribution to the cumulative PTV maps presented in the third row.

411 Presenting the GWPCA outputs for GWPCA-A and GWPCA-B with their different
412 bandwidths in this way re-affirms the findings, and quantifies how non-stationarities
413 can change at different spatial scales.

414

415 Loadings data

416 In many ways the loadings data from a GWPCA are more difficult to interpret
417 map than the scores and PTV data. In Harris, Brunsdon, and Charlton (2011), three
418 visualizations were proposed, which can only be conducted on a component by
419 component basis: (a) map the 'winning variables' - i.e. those that correspond to
420 largest absolute loading; (b) map the loading sign patterns, e.g. for eight variables,
421 there are 256 possible sign patterns; and (c) map all loadings together using
422 multivariate glyphs, where a spoke's length corresponds to the magnitude of the
423 loading, whilst a spoke's colour corresponds to the sign of the loadings. In this study,
424 the GWPCA loadings data are visualized using the first option. These 'winning year'
425 maps are presented in Figure 7 for PC1 and PC2.

426 The 'winning year' for PC1 for GWPCA-A and GWPCA-B included 15 and 17 of
427 the 23 years being selected. As so many different years 'win', this is viewed as a
428 confirmation of the generally high correlation amongst the goat population data
429 throughout the 23-year period. Differences between a year providing the highest
430 loading or not, are often extremely small. Thus a 'winning year or variable' map tends
431 to provide little useful information when this happens.

432 In this instance, greater insight stems from considering the 'winning year' maps
433 for the next component (PC2). Now far fewer years are represented (3 to 6 of 23) and
434 the dzud years of 2002 and 2010, strongly dominate in two clear regions; the west
435 and south-west, and the east and north, respectively. This suggests that: (i) the dzud
436 of 2002 and the associated goat population decline was more or less pronounced in
437 the west and south-west than elsewhere; and (ii) the dzud of 2010 and the associated
438 goat population decline was more or less pronounced in the east and north than
439 elsewhere. This strongly indicates that the severity of the dzuds in 2002 and 2010
440 varied geographically. Visualizing the annual changes in the PCA and GWPCA
441 loadings from PC1 and PC2 for GWPCA-A and GWPCA-B (Figure 8) shows the
442 effects of the 2002 and 2010 dzud years on the loadings, with clear inflection points
443 for both GWPCA fits.

444 Figure 9 displays the loadings maps for PC2 of GWPCA-A only, for 2001-3, and
445 2009-11, covering the two dzuds periods. These maps suggest that the 2001-2 dzud
446 and the 2009-10 dzud have different regional and temporal characteristics. The
447 impact of the 2001-2 dzud starts from central/western regions in 2001 and increases
448 in western regions in 2002. The impact of the 2009-10 dzud appears first in western

449 regions in 2009 and then in eastern regions in 2010. This is in contrast to the
450 reporting of dzuds and the devastating damage to livestock populations, which is
451 typically referred to as impacting Mongolia as a whole, and uniformly.

452

453 **Discussion and conclusions**

454 Understanding the spatio-temporal characteristics of livestock population
455 change is essential for environmental and disaster responses, to sustainably manage
456 grassland environments and to minimize the impact of the dzud in Mongolia.
457 Unfortunately, such analyses are rarely conducted, as they require skilled statistical
458 expertise (Cheng et al. 2014; Shekhar et al. 2015). This study undertook such an
459 analysis for annual goat population data, which are known to have increased over the
460 study period, with abrupt declines following dzud events. The application of a
461 geographically weighted PCA (GWPCA), a spatial version of PCA, to the temporally
462 indexed goat data allowed an understanding of the spatial and temporal variations in
463 goat population change across Mongolia over the 23 year study period.

464 Mapping GWPCA scores data allowed regional differences to be observed,
465 particularly in the north-eastern regions of Mongolia, bordering Russia and also

466 south-western regions bordering China. Thus the temporal dynamics of goat
467 population change is likely to be different in these regions to that expected nationally.
468 By mapping GWPCA variance proportion data, the temporal trend in goat population
469 change was found to be more uniform, to that found globally, in central northern
470 regions, whilst less uniform (to that found globally) in western regions. Visualizing the
471 'winning year' maps for the GWPCA loadings, suggests that the dzud of 2002 and the
472 associated goat population decline was more or less pronounced in the west and
473 south-west regions and that the dzud of 2010 and the associated goat population
474 decline was more or less pronounced in the east and north regions. This, in turn,
475 suggests that the dzuds of 2002 and 2010 varied geographically in their severity.

476 It has been reported that 7.7 million livestock died as a result of the 2001-2 dzud
477 and 9.7 million died as a result of the 2009-10 dzud (UNDP and NEMA 2010). This
478 study helps to re-affirm that regionally-specific dzud preparation and response
479 initiatives are required to support different landscape ecological characteristics and
480 management strategies (Fernández-Giménez et al. 2015). This study did not
481 consider change in livestock-type over space and time, and in this respect, future
482 research will seek to explore the full data set of goats, sheep, cattle, camel and horse.

483 Such an analysis could be achieved via extending GWPCA to a full temporally and
484 geographically weighted PCA form.

485 This study's application of GWPCA to temporally indexed spatial data is novel
486 and adds to a growing portfolio of GWPCA uses, not only for spatial exploration
487 (Lloyd 2010; Harris, Brunsdon, and Charlton 2011; Harris et al. 2015), but also for
488 spatial anomaly detection (Harris, Brunsdon, et al. 2014; Harris et al. 2015), spatial
489 network re-design (Harris, Clarke, et al. 2014), and spatial classification (Harris et al.
490 2015; Comber, Harris, and Tsutsumida 2016). Furthermore, this study usefully
491 extended the GWPCA methodology itself to simultaneously optimise the number of
492 components to retain and the kernel weighting bandwidth. This is considered an
493 important advance, and should be adopted in all subsequent GWPCA studies.

494

495 **Notes**

496 ¹ Observe that the current version of the GWmodel R package does not allow
497 adaptive bandwidth values greater than the sample size to be optimally selected.
498 Thus an adaptive bandwidth that is equal to the sample size only directly indicates a
499 stationary spatial process provided a box-car kernel is specified. For any

500 distance-decay kernel, such as the bi-square, an adaptive bandwidth that is equal to
501 the sample size can only suggest or allude to a stationary spatial process.

502

503 **Acknowledgements**

504 The authors would like to thank the National Statistics Office of Mongolia for providing
505 livestock population data. We appreciate Dr. Izuru Saizen and Dr. Atsushi Otomo to
506 support this work. This work was supported by Sinfonica Statistical GIS Research
507 Grants, the RIHN (project number D-04), JSPS KAKENHI Grant Number 15K21086,
508 grants for young researchers in GSGES KU, and KU SPIRITS project. For Paul
509 Harris, a UK Biotechnology and Biological Sciences Research Council grant (BBSRC
510 BB/J004308/1).

511

512 **References**

513 Cheng, T., J. Haworth, B. Anbaroglu, G. Tanaksaranond, and J. Wang. 2014.
514 Spatiotemporal Data Mining. In *Handbook of Regional Science*, eds. M. M. Fischer
515 and P. Nijkamp, 1173–1193. Berlin, Heidelberg: Springer Berlin Heidelberg
516 http://link.springer.com/10.1007/978-3-642-23430-9_68.

- 517 Comber, A. J., P. Harris, and N. Tsutsumida. 2016. Improving land cover
518 classification using input variables derived from a geographically weighted principal
519 components analysis. *ISPRS Journal of Photogrammetry and Remote Sensing*
520 119:347–360. <http://linkinghub.elsevier.com/retrieve/pii/S0924271616301290>.
- 521 Demšar, U., P. Harris, C. Brunsdon, A. S. Fotheringham, and S. McLoone. 2013.
522 Principal Component Analysis on Spatial Data: An Overview. *Annals of the*
523 *Association of American Geographers* 103 (1):106–128.
524 <http://www.tandfonline.com/doi/abs/10.1080/00045608.2012.689236>.
- 525 Felipe-Sotelo, M., L. Gustems, I. Hernández, M. Terrado, and R. Tauler. 2006.
526 Investigation of geographical and temporal distribution of tropospheric ozone in
527 Catalonia (North-East Spain) during the period 2000-2004 using multivariate data
528 analysis methods. *Atmospheric Environment* 40 (38):7421–7436.
- 529 Fernandez-Gimenez, M. E. 2006. Land Use and Land Tenure in Mongolia : A Brief
530 History and Current Issues. In *Rangelands of Central Asia: Proceedings of the*
531 *Conference on Transformations, Issues, and Future Challenges*, eds. D. J. Bedunah,
532 E. D. McArthur, and M. E. Fernandez-Gimenez, 30–36. Salt Lake City: U.S.
533 Department of Agriculture, Forest Service, Rocky Mountain Research Station.

- 534 Fernandez-Gimenez, M. E., B. Batbuyan, and B. Baival. 2012. *Lessons from the*
535 *Dzud: Adaptation and Resilience in Mongolian Pastoral Social-Ecological Systems.*
536 The world bank.
537 <http://www.worldbank.org/en/news/feature/2012/11/06/lessons-from-dzud>.
- 538 Fernández-Giménez, M. E., B. Batkhisig, and B. Batbuyan. 2012. Cross-boundary
539 and cross-level dynamics increase vulnerability to severe winter disasters (dzud) in
540 Mongolia. *Global Environmental Change* 22 (4):836–851.
541 <http://linkinghub.elsevier.com/retrieve/pii/S0959378012000684>.
- 542 Fernández-Giménez, M. E., B. Batkhisig, B. Batbuyan, and T. Ulambayar. 2015.
543 Lessons from the Dzud: Community-Based Rangeland Management Increases the
544 Adaptive Capacity of Mongolian Herders to Winter Disasters. *World Development*
545 68:48–65.
- 546 Fotheringham, A. S., C. Brunson, and M. Charlton. 2002. *Geographically weighted*
547 *regression: the analysis of spatially varying relationships*. Chichester: Wiley.
- 548 Geist, H. J., and E. F. Lambin. 2004. Dynamic Causal Patterns of Desertification.
549 *BioScience* 54 (9):817.
550 [https://academic.oup.com/bioscience/article-lookup/doi/10.1641/0006-3568\(2004\)05](https://academic.oup.com/bioscience/article-lookup/doi/10.1641/0006-3568(2004)05)

551 4[0817:DCPOD]2.0.CO;2.

552 Gollini, I., B. Lu, M. Charlton, C. Brunsdon, and P. Harris. 2015. GWmodel : An R

553 Package for Exploring Spatial Heterogeneity Using Geographically Weighted Models.

554 *Journal of Statistical Software* 63 (17):85–101.

555 <http://www.tandfonline.com/doi/abs/10.1080/10095020.2014.917453>.

556 Harris, P., and C. Brunsdon. 2010. Exploring spatial variation and spatial

557 relationships in a freshwater acidification critical load data set for Great Britain using

558 geographically weighted summary statistics. *Computers & Geosciences* 36 (1):54–70.

559 <http://dx.doi.org/10.1016/j.cageo.2009.04.012>.

560 Harris, P., C. Brunsdon, and M. Charlton. 2011. Geographically weighted principal

561 components analysis. *International Journal of Geographical Information Science* 25

562 (10):1717–1736.

563 <http://www.tandfonline.com/doi/abs/10.1080/13658816.2011.554838>.

564 Harris, P., C. Brunsdon, M. Charlton, S. Juggins, and A. Clarke. 2014. Multivariate

565 Spatial Outlier Detection Using Robust Geographically Weighted Methods.

566 *Mathematical Geosciences* 46 (1):1–31.

567 <http://link.springer.com/10.1007/s11004-013-9491-0>.

- 568 Harris, P., A. Clarke, S. Juggins, C. Brunsdon, and M. Charlton. 2014. Geographically
569 weighted methods and their use in network re-designs for environmental monitoring.
570 *Stochastic Environmental Research and Risk Assessment* 28 (7):1869–1887.
571 <http://link.springer.com/10.1007/s00477-014-0851-1>.
- 572 ———. 2015. Enhancements to a Geographically Weighted Principal Component
573 Analysis in the Context of an Application to an Environmental Data Set. *Geographical*
574 *Analysis* 47 (2):146–172. <http://doi.wiley.com/10.1111/gean.12048>.
- 575 Huang, B., B. Wu, and M. Barry. 2010. Geographically and temporally weighted
576 regression for modeling spatio-temporal variation in house prices eds. M. M. Fischer
577 and P. Nijkamp. *International Journal of Geographical Information Science* 24
578 (3):383–401. <http://link.springer.com/10.1007/978-3-642-23430-9> (last accessed 11
579 July 2014).
- 580 Lasaponara, R. 2006. On the use of principal component analysis (PCA) for
581 evaluating interannual vegetation anomalies from SPOT/VEGETATION NDVI
582 temporal series. *Ecological Modelling* 194 (4):429–434.
583 <http://linkinghub.elsevier.com/retrieve/pii/S0304380005005454> (last accessed 5 April
584 2012).

- 585 Lloyd, C. D. 2010. Analysing population characteristics using geographically
586 weighted principal components analysis: A case study of Northern Ireland in 2001.
587 *Computers, Environment and Urban Systems* 34 (5):389–399.
588 <http://dx.doi.org/10.1016/j.compenvurbsys.2010.02.005>.
- 589 Lu, B., P. Harris, M. Charlton, and C. Brunsdon. 2014. The GWmodel R package:
590 further topics for exploring spatial heterogeneity using geographically weighted
591 models. *Geo-spatial Information Science* 17 (2):85–101.
592 <http://www.tandfonline.com/doi/abs/10.1080/10095020.2014.917453>.
- 593 Millennium Ecosystem Assessment. 2005. *Ecosystems and Human Well-being:*
594 *Desertification Synthesis*. Washington, D.C.
595 <http://library.wur.nl/WebQuery/clc/1785684>.
- 596 Obled, C., and J. D. Creutin. 1986. Some Developments in the Use of Empirical
597 Orthogonal Functions for Mapping Meteorological Fields. *Journal of Climate and*
598 *Applied Meteorology* 25 (9):1189–1204.
599 <http://journals.ametsoc.org/doi/abs/10.1175/1520-0450%281986%29025%3C1189%3ASDITUO%3E2.0.CO%3B2>.
- 600
601 Research Institute for Humanity and Nature. 2012. *Collapse and restoration of*

- 602 *ecosystem networks with human activity*. Kyoto.
- 603 Saizen, I., A. Maekawa, and N. Yamamura. 2010. Spatial analysis of time-series
604 changes in livestock distribution by detection of local spatial associations in Mongolia.
605 *Applied Geography* 30 (4):639–649.
606 <http://linkinghub.elsevier.com/retrieve/pii/S0143622810000032> (last accessed 6
607 August 2011).
- 608 Shekhar, S., Z. Jiang, R. Ali, E. Eftelioglu, X. Tang, V. Gunturi, and X. Zhou. 2015.
609 Spatiotemporal Data Mining: A Computational Perspective. *ISPRS International*
610 *Journal of Geo-Information* 4 (4):2306–2338.
611 <http://www.mdpi.com/2220-9964/4/4/2306/>.
- 612 Stacklies, W., H. Redestig, M. Scholz, D. Walther, and J. Selbig. 2007. pcaMethods a
613 bioconductor package providing PCA methods for incomplete data. *Bioinformatics* 23
614 (9):1164–1167.
615 <https://academic.oup.com/bioinformatics/article-lookup/doi/10.1093/bioinformatics/btm069>.
616 m069.
- 617 Suttie, J. M., S. G. Reynolds, and C. Batello. 2005. *Grasslands of the world* eds. J. .
618 Suttie, S. G. Reynolds, and C. Batello. Rome: Food and Agriculture Organization.

619 Togtokh, C. 2008. Climate change adaptation strategies for pastoral communities of
620 Mongolia's central mountainous region. *IHDP Update* :53–58.

621 Tsutsumida, N., and I. Saizen. 2014. Internal Regional Migration Analysis and
622 Modeling of Population Concentration for Ulaanbaatar, Mongolia. *Papers on*
623 *Environmental Information Science* 28:25–30.

624 UNDP and NEMA. 2010. *Dzud national report 2009-2010*.

625 Varmuza, K., and P. Filzmoser. 2009. *Introduction to multivariate statistical analysis*
626 *in chemometrics*. Taylor & Francis.

627

628

629 **Author professional/contact information**

630 NARUMASA TSUTSUMIDA is an Assistant Professor in the Graduate School of
631 Global Environmental Studies at Kyoto University, Yoshida-honmachi, Sakyo, Kyoto,
632 JP 606-8501. E-mail: naru@kais.kyoto-u.ac.jp. His research interests include the
633 application of geographical information in the field of environmental studies.

634 PAUL HARRIS is a Senior Research Scientist at Rothamsted Research, North Wyke,
635 Okehampton, Devon, UK EX20 2SB, Email: paul.harris@rothamsted.ac.uk. His
636 research focuses on the development and application of spatial statistics to
637 agricultural, ecological and environmental data.

638 ALEXIS COMBER holds a chair in Spatial Data Analytics in the School of Geography
639 at University of Leeds, Leeds, UK LS2 9JT, Email: a.comber@leeds.ac.uk. His
640 research develops methods to integrate and analyse high volumes of spatial data to
641 uncover hidden patterns with applications in environmental, socio-economic and
642 public health areas.

643

644

645

646

647 **Figure captions**

648 Figure 1. Change in livestock populations across Mongolia during 1990–2012.

649

650 Figure 2. Correlation matrix of annual goat population data (1990-2012), with the plot
651 size proportional to the correlation.

652

653 Figure 3. GW correlation maps between PC1-3 scores of the global PCA and the raw
654 data of the corresponding most influential years (see also Table 2).

655

656 Figure 4. GWPCA calibration: (i) GoF (via LOOR CoV) versus NCR values; and (ii)
657 scree plots for local cumulative PTVs versus NCR values. The grey lines have a
658 transparency term added to them. In (i) they represent bandwidths in a range of 5 to
659 341 and (ii) in a range of 10 to 341. The black line in (i) represents the optimal
660 bandwidth of 247 with NCR = 5, at the minimum GoF. Black line in (ii) represents the
661 90% threshold of the cumulative PTV.

662

663 Figure 5. PC1 and PC2 scores maps for GWPCA-A (top row), GWPCA-B (middle
664 row), and the global PCA (bottom row).

665

666 Figure 6. GWPCA-A and GWPCA-B PTV maps for PC1 (top row), PC2 (middle row)
667 and PC1/PC2 combined (bottom row).

668

669 Figure 7. GWPCA-A and GWPCA-B 'winning year' maps (by highest loadings) for
670 PC1 and PC2. Years when dzud occurred are highlighted in grey and black.

671

672 Figure 8. GWPCA-A and GWPCA-B loadings for PC1 and PC2, displayed over the 23
673 study years. The grey lines have a transparency term and represent the loading score
674 at every soum. The black lines represent the loadings from the global PCA. Dark grey
675 rectangles represent dzud periods 2001-2 and 2009-10.

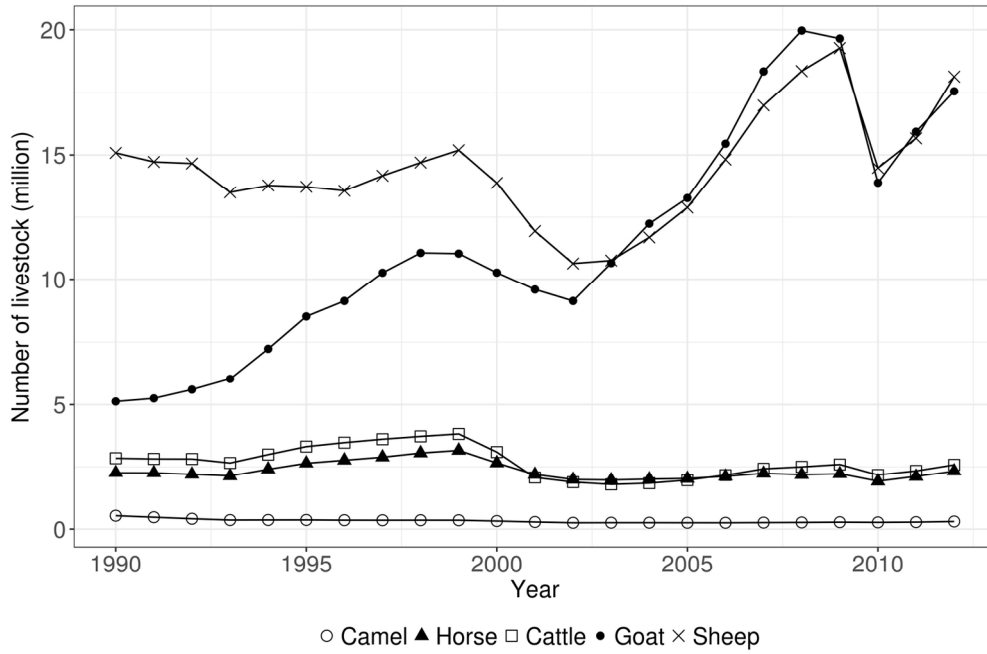
676

677 Figure 9. Maps for PC2 loadings from GWPCA-A over dzud periods of 2001-3 (top
678 row) and 2009-11 (bottom row).

679

680

For Peer Review Only

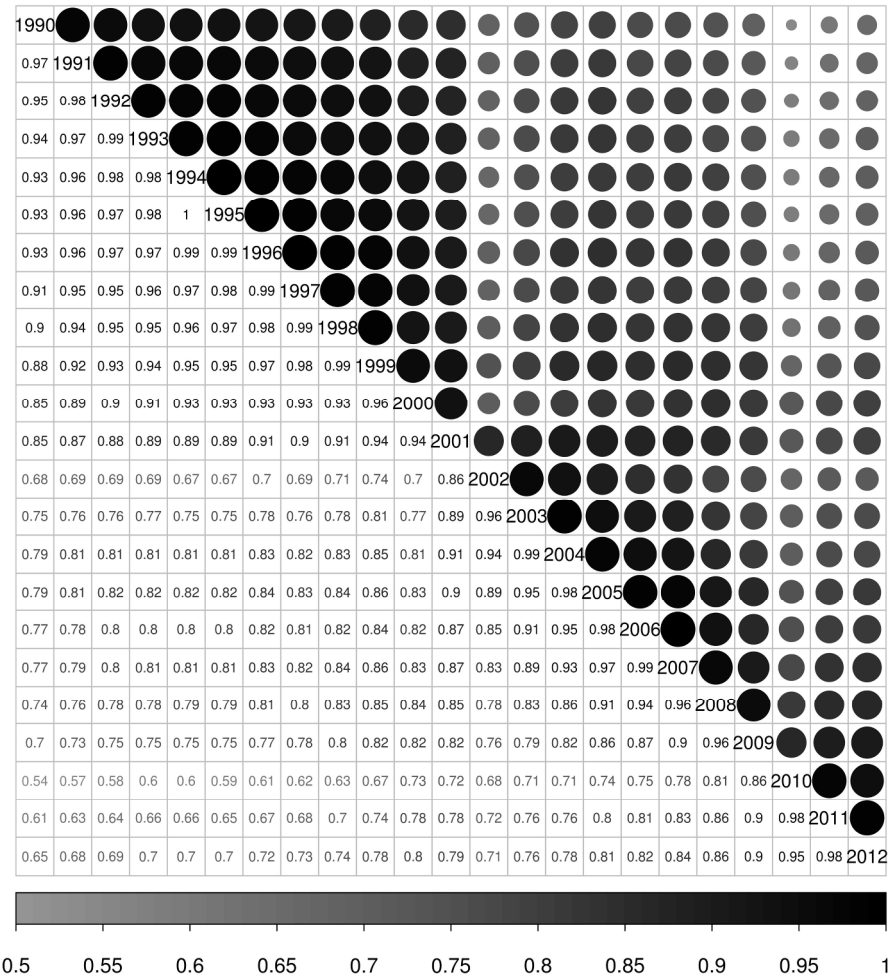


Change in livestock populations across Mongolia during 1990–2012.

Figure 1

152x101mm (300 x 300 DPI)

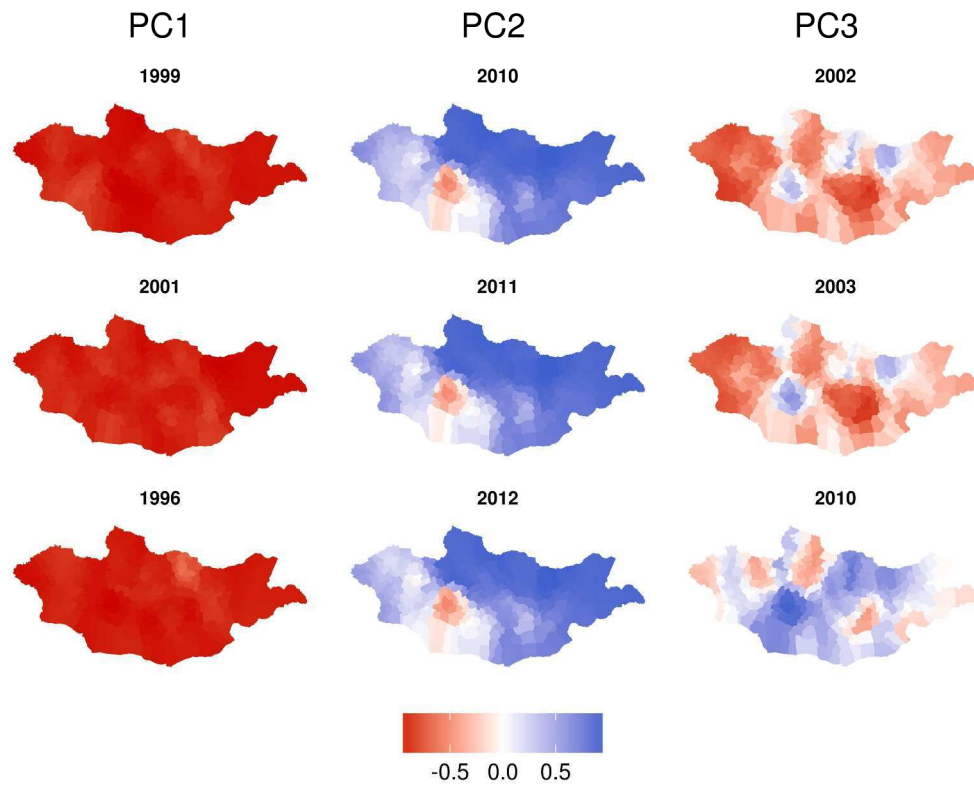
view Only



Correlation matrix of annual goat population data (1990-2012), with the plot size proportional to the correlation.

Figure 2
228x228mm (300 x 300 DPI)

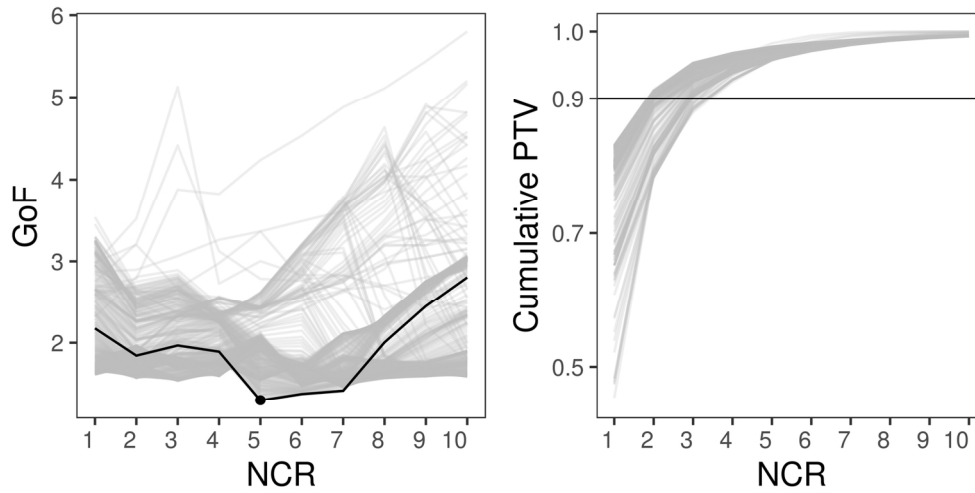




GW correlation maps between PC1-3 scores of the global PCA and the raw data of the corresponding most influential years (see also Table 2).

Figure 3
127x105mm (600 x 600 DPI)

Only

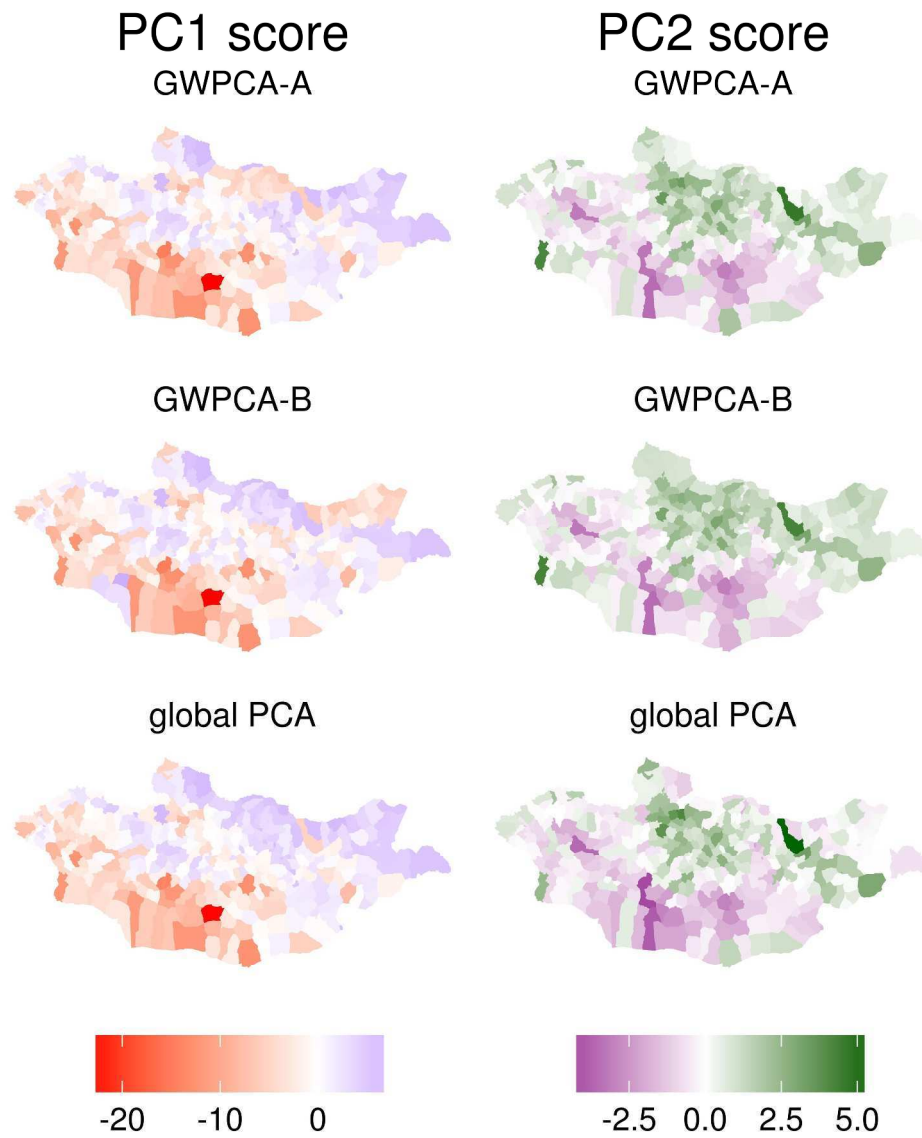


GWPCA calibration: (i) GoF (via LOOR CoV) versus NCR values; and (ii) scree plots for local cumulative PTVs versus NCR values. The grey lines have a transparency term added to them. In (i) they represent bandwidths in a range of 5 to 341 and (ii) in a range of 10 to 341. The black line in (i) represents the optimal bandwidth of 247 with $NCR = 5$, at the minimum GoF. Black line in (ii) represents the 90% threshold of the cumulative PTV.

Figure 4

76x38mm (600 x 600 DPI)

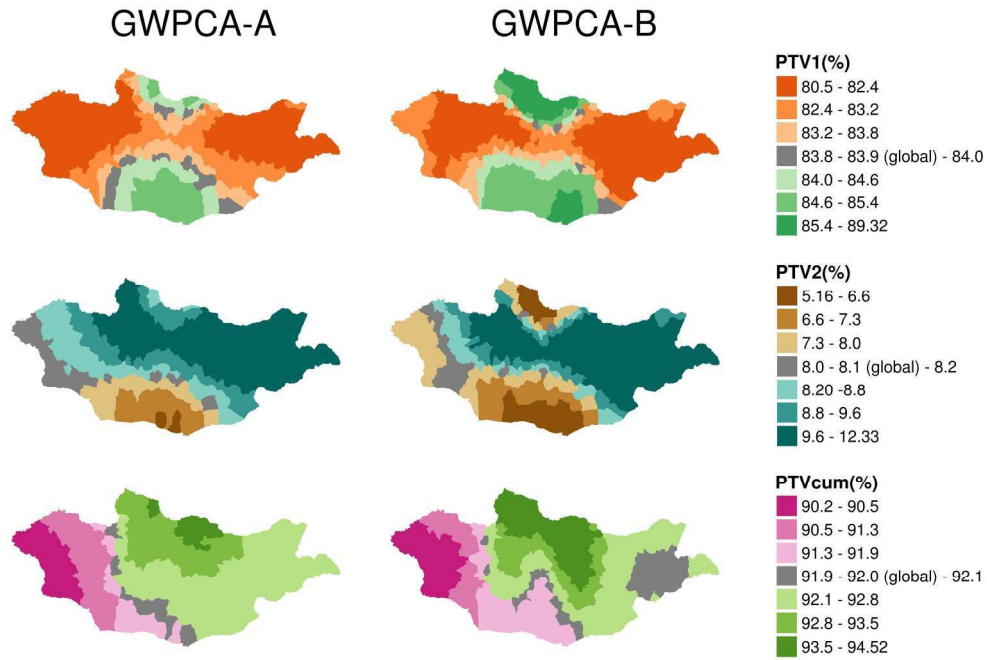
Review Only



PC1 and PC2 scores maps for GWPCA-A (top row), GWPCA-B (middle row), and the global PCA (bottom row).

Figure 5

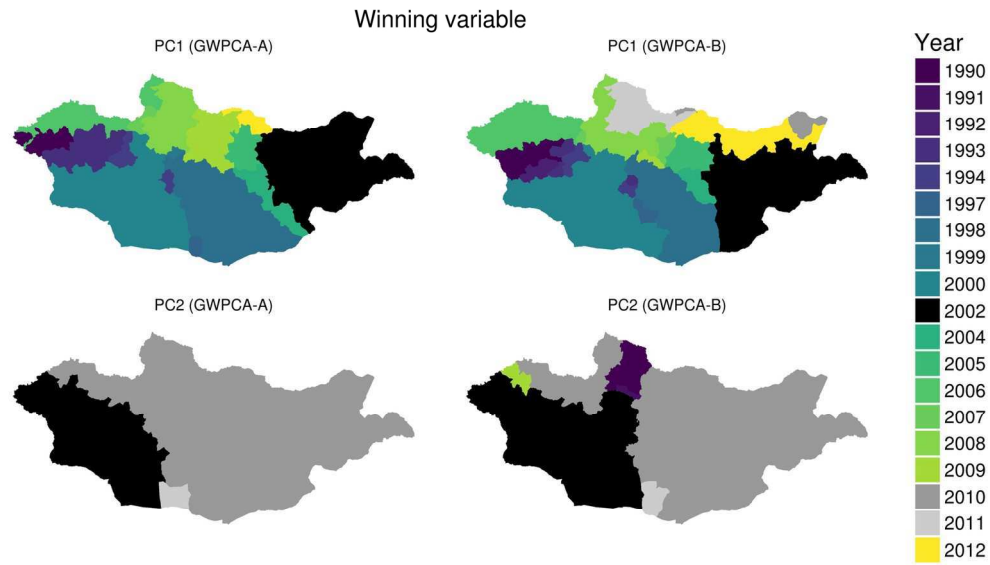
127x158mm (600 x 600 DPI)



GWPCA-A and GWPCA-B PTV maps for PC1 (top row), PC2 (middle row) and PC1/PC2 combined (bottom row).

Figure 6
 101x67mm (600 x 600 DPI)

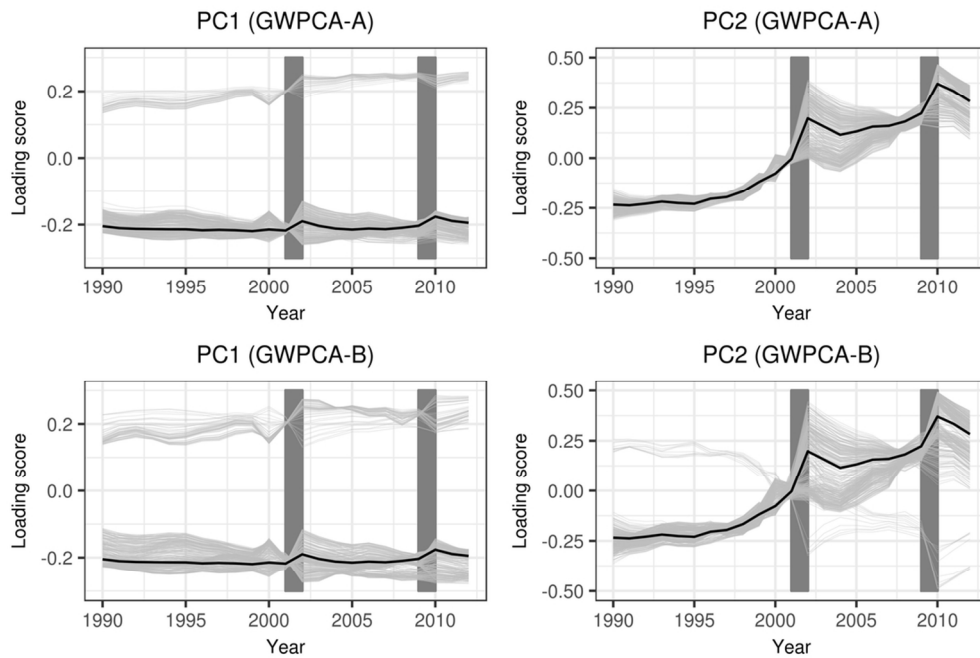
View Only



GWPCA-A and GWPCA-B 'winning year' maps (by highest loadings) for PC1 and PC2. Years when dzud occurred are highlighted in grey and black.

Figure 7
152x101mm (300 x 300 DPI)

View Only

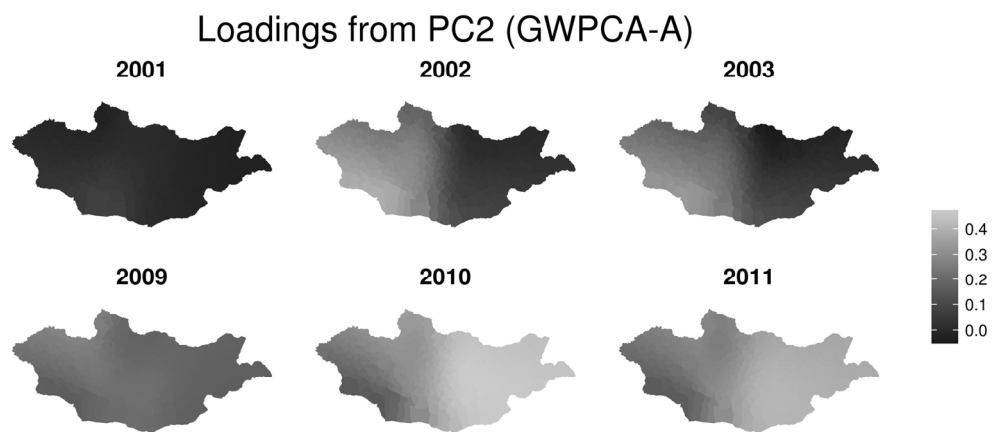


GWPCA-A and GWPCA-B loadings for PC1 and PC2, displayed over the 23 study years. The grey lines have a transparency term and represent the loading score at every soum. The black lines represent the loadings from the global PCA. Dark grey rectangles represent dzud periods 2001-2 and 2009-10.

Figure 8

101x67mm (300 x 300 DPI)

ew Only



Maps for PC2 loadings from GWPCA-A over dzud periods of 2001-3 (top row) and 2009-11 (bottom row).

Figure 9

76x38mm (600 x 600 DPI)

Review Only

Tables

Table 1. Eigenvalues, PTV, and cumulative PTV for the global PCA. Only the first 5 PCs are shown.

	PC1	PC2	PC3	PC4	PC5
Eigenvalues	4.39	1.36	0.90	0.56	0.46
PTV (%)	83.86	8.09	3.56	1.37	0.91
Cumulative PTV (%)	83.86	91.95	95.51	96.88	97.78

Table 2. Loadings for the first five PCs of the global PCA ordered by contribution.

	PC1	PC2	PC3	PC4	PC5
1st	1999 (-0.220)	2010 (0.371)	2002 (-0.446)	2008 (0.446)	1990 (0.495)
2nd	2001 (-0.218)	2011 (0.334)	2003 (-0.388)	2007 (0.396)	2000 (-0.383)
3rd	1996 (-0.217)	2012 (0.283)	2010 (0.352)	2002 (-0.354)	1999 (-0.346)
4th	1998 (-0.217)	1991 (-0.237)	2004 (-0.341)	2006 (0.351)	2001 (-0.337)
5th	1997 (-0.216)	1990 (-0.234)	2012 (0.371)	2009 (0.269)	1991 (0.327)

Table 3. GWPCA calibration: optimum adaptive bandwidths for different values of NCR.

NCR	1	2	3	4	5	6	7	8	9	10
Bandwidth	341	341	284	277	341	341	341	341	341	341

For Peer Review Only